Direct Motion Estimation from a Range Scan Sequence

Javier Gonzalez
Departamento de Ingenieria de Sistemas y Automatica
University of Malaga
Campus Teatinos
29080 Malaga, Spain
e-mail: jgonzalez@ctima.uma.es

Rafael Gutierrez
Departamento de Electronica
University of Jaen
Alfonso X El Sabio
23700 Linares, Spain
e-mail: rgutierr@piturda.ujaen.es

Received December 2, 1997; accepted October 8, 1998

This article presents an innovative method to estimate the motion parameters of a mobile robot equipped with a radial laser range-finder. Our approach is based on the spatial and temporal linearization of the range function, which leads to a velocity constraint equation for the scanned points. Assuming that the mobile robot moves in a rigid environment, a least-squares formulation is employed to come up with the motion estimation as well as the motion vectors of the scanned points as they move from scan to scan in the sequence. This motion field can be very useful for a number of applications including detection and tracking of moving objects. Although this is a preliminary work, experimental results show that good results are achieved with both real and synthetic data.

1. INTRODUCTION

We consider the problem of estimating the instantaneous motion parameters of a mobile robot from a scan sequence provided by a radial laser range-finder. Basically, such a sensor consists of a pulsed infrared laser transmitter/receiver pair and a mirror that rotates about the vertical axis to deflect the laser beam so that it emerges parallel to the ground (Figure 1). By recording the amount of time it takes for a transmitter pulse to bounce off a target and be detected by the receiver, the scanner provides a

CCC 0741-2223/99/020073-08

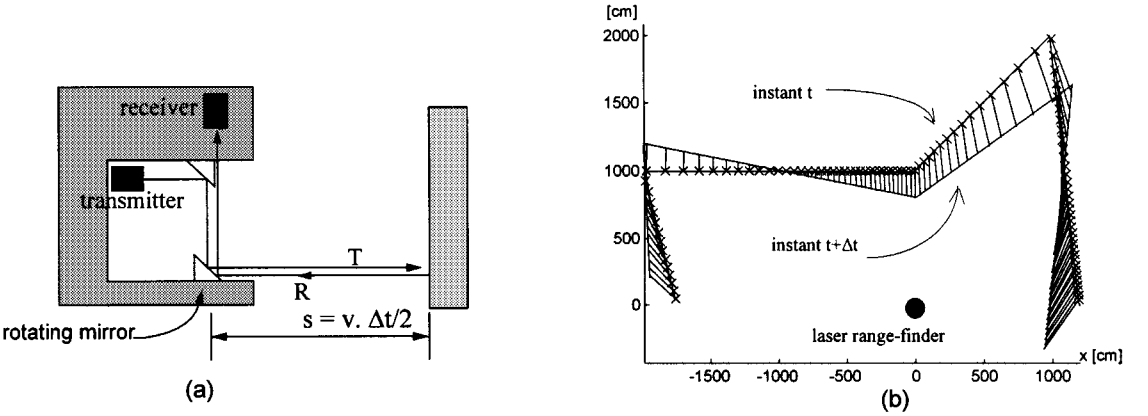

Figure 1. (a) A schematic representation of a typical radial laser range-finder. (b) Velocity field due to a translation and rotation of the radial laser scanner. For the sake of clarity, the motion field has been magnified and the scanner remains static [at the position (0, 0)] while the environment moves.

two-dimensional (polar) representation of the environment. The field of view used varies from 180 to 360°. Other characteristics, including accuracy, points per revolution, resolution, maximum and minimum range, scanning speed, etc., depend on the kind of sensor.

The formulation we present here is based on computing the motion field that arises in a range scan when the sensor moves relative to the environment. A vector in this field indicates the motion of each range point between consecutive scans. In our study, we assume that the environment is rigid, that is, it remains static while the sensor moves. Figure 2 shows the environment at two instants of time and the motion field for some of the scanned points.

The problem of recovering the motion parameters can be formulated as that of matching two consecutive scans of the sequence provided by the scanner. This problem has a great importance in the mobile robot context, including pose estimation and

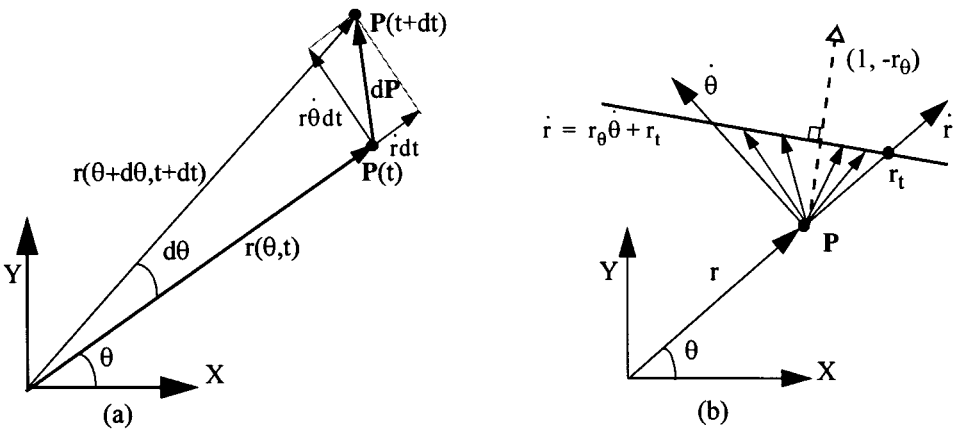

Figure 2. (a) Motion of a point in polar coordinates. (b) A visual interpretation of the velocity constraint equation.

map building. Three different approaches were previously proposed to do this:

1. *Feature to feature correspondence*. Registration of the two scans is accomplished by first extracting a set of features (usually segments and corners) and then making correspondences between pairs of features of the two scans. Some examples of this approach are the works presented by Shaffer[1] for mobile robot pose estimation and Gonzalez et al.[2] for map building.
2. *Point to feature correspondence*. The range points of the scan are matched against features of a model or of a map obtained from previous scans. The position estimation algorithms proposed by Cox[3] and Gonzalez et al.[4] are some examples of this approach.
3. *Point to point correspondence*. This scheme intends to match one range scan to another to derive the relative robot pose. The registration is accomplished without explicitly using the underlying features that exist in the scans. A notable example is the iterative dual correspondence algorithm developed by Lu.[5] The algorithm we propose falls into this category.

Lu's algorithm establishes correspondences for data points by combining two rules: a *closest-point rule*, which chooses the closest point in the next scan as the correspondence for the data point, and a *matching-range-point rule*, which assumes there is no translation between the two scans and chooses, for correspondence, the closest point with the same range. Our approach avoids solving for the correspondences of the range points. It is inspired by the ''optical flow constraint equation'' developed by Horn and Schunck[6] for brightness images and states that the velocity of a range point is restricted by the local structure of the environment as well as its temporal rate of change. We believe that Lu's approach may be more effective than ours for pose estimation problems; however, our method is more appropriate to detect and track moving objects.

In the following sections we first derive the equations of the relative motion of a radial rangefinder in a rigid environment. In section 3, the equation that constrains the motion of each scanned point is presented. Next, the formulation for estimating the motion field along with the motion parameters of the sensor is proposed. In section 5, the implementation details are presented. In section 6, some experimental results with both real and synthetic data are shown. We end with some conclusions and future work.

2. MOTION OF A TWO-DIMENSIONAL RANGE SCANNER IN A RIGID ENVIRONMENT

Let $\mathbf{V}$ and $\mathbf{W}$ be the translational and rotational velocity vectors of a two-dimensional (2-D) range scanner moving on a flat surface. A point $\mathbf{P}$ from the environment seems to move relative to the sensor with instantaneous velocity $\mathbf{V_P}$ given by

$$\mathbf{V_P} = -\mathbf{W} \times \mathbf{P} - \mathbf{V} = -\begin{bmatrix} 0 \\ 0 \\ w \end{bmatrix} \times \begin{bmatrix} r\cos\theta \\ r\sin\theta \\ 0 \end{bmatrix} - \begin{bmatrix} u \\ v \\ 0 \end{bmatrix}$$

where $[r, \theta]^T$ are the polar coordinates of the point $\mathbf{P}$. Since the third component of this equation is meaningless, it can be eliminated:

$$\mathbf{V_P} = -wr\begin{bmatrix} -\sin\theta \\ \cos\theta \end{bmatrix} - \begin{bmatrix} u \\ v \end{bmatrix} \tag{1}$$

On the other hand, since the velocity of the point $\mathbf{P}$ is the derivative of $\mathbf{P}$ with respect to time, we have

$$\mathbf{V_P} = \frac{d\mathbf{P}}{dt} = \frac{d}{dt}\begin{bmatrix} r\cos\theta \\ r\sin\theta \end{bmatrix} = \begin{bmatrix} \dot{r}\cos\theta - r\dot{\theta}\sin\theta \\ \dot{r}\sin\theta + r\dot{\theta}\cos\theta \end{bmatrix}$$
$$= \begin{bmatrix} \cos\theta & -r\sin\theta \\ \sin\theta & r\cos\theta \end{bmatrix}\begin{bmatrix} \dot{r} \\ \dot{\theta} \end{bmatrix} = \mathbf{J}\begin{bmatrix} \dot{r} \\ \dot{\theta} \end{bmatrix} \tag{2}$$

where $\mathbf{J}$ is the Jacobian of the transformation from polar to Cartesian coordinates and $[r, \theta]^T$ is the *polar velocity vector* of the point $\mathbf{P}$ (see Figure 2).

From Eqs. (1) and (2), we get

$$\begin{bmatrix} \cos\theta & -r\sin\theta \\ \sin\theta & r\cos\theta \end{bmatrix}\begin{bmatrix} \dot{r} \\ \dot{\theta} \end{bmatrix} + wr\begin{bmatrix} \sin\theta \\ \cos\theta \end{bmatrix} + \begin{bmatrix} u \\ v \end{bmatrix} = 0 \tag{3}$$

This expression holds for any point $\mathbf{P}$ from the scene and consists of two linear equations with five unknowns: the mobile robot motion parameters (u, v, w) and the velocity vector $[\dot{r}, \dot{\theta}]^T$. By considering the n points of a scan taken in a rigid environment, we would obtain an underconstrained system with $2n$ equations and $2n + 3$ unknowns. Consequently, some additional constraints are required to solve for the motion parameters.

3. THE VELOCITY CONSTRAINT EQUATION

Although neither $\dot{r}$ nor $\dot{\theta}$ can be estimated from the range scan, it is possible to establish a relationship between them by taking into account the information provided by a range scan sequence. Let $r(\theta, t)$ be the range measured for a generic point **P** at scan angle θ and time t. Assuming the derivability of $r(\theta, t)$, at some later time $t + dt$, the point **P** will be scanned at an angle $\theta + d\theta$ with the range

$$r(\theta + d\theta, t + dt) = r(\theta, t) + \frac{\partial r}{\partial \theta} d\theta + \frac{\partial r}{\partial t} dt + O(e) \tag{4}$$

where $O(e)$ denotes the higher order terms in $d\theta$ and dt. Subtracting $r(\theta, t)$ from both sides of Eq. (4), dividing through by dt, and taking the limit $dt \to 0$, we obtain

$$\dot{r} = \frac{d}{dt} r(\theta, t) = \frac{\partial r}{\partial \theta} \frac{d\theta}{dt} + \frac{\partial r}{\partial t} = r_\theta \dot{\theta} + r_t \tag{5}$$

where r_θ and r_t are the partial derivatives of the range function with respect to the angle θ and time t, respectively, which can be estimated from the range scan sequence. Notice that Eq. (5) is no longer valid at those range points where the angular and temporal smoothness of the function $r(\theta, t)$ is violated; that is, near the corners. This turns out to be a minor limitation as long as the displacements between scans are kept small or there are very few corners in the environment.

The important point here is that Eq. (5) states a constraint over the possible velocities that a point $[r, \theta]^T$ from the scene can reach once the local structure of the environment (r_θ) and its temporal rate of change (r_t) have been estimated. We call this equation the *velocity constraint equation*, which in the polar velocity space $(\dot{r} - \theta)$ represents a line with slope r_θ and ordinate at the origin r_t (as graphically illustrated in Figure 2b). Thus, assuming that r_θ and r_t are known at a given instant of time t and angle θ, the polar velocity vector of the scanned point at θ cannot be arbitrary: its component in the direction $[1, -r_\theta]^T$ (perpendicular to the surface) is

$$\frac{-r_t}{(1 + r_\theta^2)^{1/2}}$$

However, the component of the velocity vector in the direction tangent to the object cannot be determined. Notice the analogy with the *aperture problem* reported by Horn and Schunck[6] for the optical flow in brightness images.

4. ESTIMATING THE MOTION PARAMETERS AND SOLVING FOR THE MOTION FIELD

The formulation we derive here is somehow similar to that reported by Horn and Negahdaripour[7] for direct passive navigation. In our case, however, it is not necessary to incorporate physical constraints like planar or quadratic surfaces into the formulation.

According to Eq. (5), the polar velocity vector has only 1 degree of freedom, for example, $\dot{\theta}$ and can be expressed as

$$\begin{bmatrix} \dot{r} \\ \dot{\theta} \end{bmatrix} = \begin{bmatrix} r_\theta \dot{\theta} + r_t \\ \dot{\theta} \end{bmatrix} = \begin{bmatrix} r_\theta \\ 1 \end{bmatrix} \dot{\theta} + \begin{bmatrix} r_t \\ 0 \end{bmatrix} = \mathbf{R}_\theta \dot{\theta} + \mathbf{R}_t \tag{6}$$

From Eqs. (3) and (6), we obtain two linear equations for the unknowns $\dot{\theta}, w, u, v$:

$$\mathbf{J}\mathbf{R}_\theta \dot{\theta} + \mathbf{J}\mathbf{R}_t + wr \begin{bmatrix} -\sin\theta \\ \cos\theta \end{bmatrix} + \begin{bmatrix} u \\ v \end{bmatrix} = 0 \tag{7}$$

This equation has still 2 degrees of freedom. Since each scanned point provides two additional constraints and only one additional unknown (its angular velocity $\dot{\theta}$), a minimum of three scanned points will suffice to solve for the six unknowns $(\dot{\theta}_1, \dot{\theta}_2, \dot{\theta}_3, w, u, v)$.

In practice, the solution obtained by using the minimum number of points (i.e., equations) is noisy because of noise in the range scans, quantization errors, and errors in estimate derivatives using finite difference methods. By considering n scanned points, the total number of equations becomes $2n$, while the number of unknowns is $n + 3$. This leads to a least-squares formulation that allows us to recover more robustly and accurately the robot motion parameters. This formulation will be derived in detail in the next section.

5. IMPLEMENTATION

To apply the proposed formulation to a range scan sequence, we need to formulate Eq. (7) in a discrete fashion as well as to combine in a matrix form all the equations provided by the points being consid-

ered. Let r_k be the range at the discrete angle θ_k. Also, using the subscript k to denote the fact that the functions are evaluated at the discrete angle θ_k, Eq. (7) can be rewritten

$$\mathbf{J}_k(\mathbf{R}_\theta)_k\dot{\theta}_k + \mathbf{J}_k(\mathbf{R}_t)_k + wr_k\begin{bmatrix}-\sin\theta_k\\ \cos\theta_k\end{bmatrix} + \begin{bmatrix}u\\ v\end{bmatrix} = 0 \quad (8)$$

where the partial derivatives $(r_\theta)_k$ and $(r_t)_k$ in $(\mathbf{R}_\theta)_k$ and $(\mathbf{R}_t)_k$, respectively, can be estimated from the range scan sequence using numerical differentiations[8]

$$(r_\theta)_k = \frac{r_{k+1}(t) - r_{k-1}(t)}{2\,\Delta\theta}$$

$$(r_t)_k = \frac{r_k(t) - r_k(t-\Delta t)}{\Delta t}$$

with Δt being the time between consecutive scans. Whereas a 2D laser range sensor scans radially at a fixed angular increment, we have $\Delta\theta = \theta_k - \theta_{k-1} =$ constant for any value of k.

Equation (8) can be rewritten more conveniently in the form

$$[\mathbf{J}_k(\mathbf{R}_\theta)_k \quad \mathbf{I} \quad \mathbf{Q}_k]\begin{bmatrix}\dot{\theta}_k\\ u\\ v\\ w\end{bmatrix} = -\mathbf{J}_k(\mathbf{R}_t)_k \quad (9)$$

where $\mathbf{I}$ is the 2×2 identity matrix and $\mathbf{Q}_k = [-r_k\sin\theta_k\ r_k\cos\theta_k]^T$.

Let $\{r_k,\ k = 1,\ldots,n\}$ be a range image taken at time t. Since each range r_k gives rise to a pair of equations (9), we obtain the following system of $2n$ linear equations and $n+3$ unknowns:

$$\begin{bmatrix}\mathbf{J}_1(\mathbf{R}_\theta)_1 & 0 & \cdots & 0 & \mathbf{I} & \mathbf{Q}_1\\ 0 & \mathbf{J}_2(\mathbf{R}_\theta)_2 & \cdots & 0 & \mathbf{I} & \mathbf{Q}_2\\ \vdots & \vdots & \vdots & \vdots & \vdots & \vdots\\ 0 & 0 & \cdots & \mathbf{J}_n(\mathbf{R}_\theta)_n & \mathbf{I} & \mathbf{Q}_n\end{bmatrix} \times \begin{bmatrix}\dot{\theta}_1\\ \dot{\theta}_2\\ \vdots\\ \dot{\theta}_n\\ u\\ v\\ w\end{bmatrix} = -\begin{bmatrix}\mathbf{J}_1(\mathbf{R}_t)_1\\ \mathbf{J}_2(\mathbf{R}_t)_2\\ \vdots\\ \mathbf{J}_n(\mathbf{R}_t)_n\end{bmatrix} \quad (10)$$

Since the system is overconstrained, Eq. (10) is solved through a least-squares solution

$$\mathbf{X} = (\mathbf{A}^T\mathbf{A})^{-1}\mathbf{A}^T\mathbf{B}$$

where $\mathbf{A}$ is the $2n\times n+3$ matrix on the left side of Eq. (10), $\mathbf{X}$ is the unknown vector, and $\mathbf{B}$ is the vector on the right. Notice that the number of points n in a scan may be up to several hundreds or even thousands, which makes it computationally prohibitive to invert the matrix $\mathbf{A}^T\mathbf{A}$, which dimension is $n+3xn+3$. Fortunately, it is a really special matrix that besides being symmetric is mostly diagonal. Thus, to find the inverse of matrix $\mathbf{A}^T\mathbf{A}$, we can decompose as[9]

$$(\mathbf{A}^T\mathbf{A})^{-1} = \begin{bmatrix}\mathbf{M} & \mathbf{N}\\ \mathbf{O} & \mathbf{P}\end{bmatrix}^{-1} = \begin{bmatrix}\mathbf{M}^{-1} + \mathbf{M}^{-1}\mathbf{N}(\mathbf{P}-\mathbf{O}\mathbf{M}^{-1}\mathbf{N})^{-1}\mathbf{O}\mathbf{M}^{-1} & -\mathbf{M}^{-1}\mathbf{N}(\mathbf{P}-\mathbf{O}\mathbf{M}^{-1}\mathbf{N})^{-1}\\ -(\mathbf{P}-\mathbf{O}\mathbf{M}^{-1}\mathbf{N})^{-1}\mathbf{O}\mathbf{M}^{-1} & (\mathbf{P}-\mathbf{O}\mathbf{M}^{-1}\mathbf{N})^{-1}\end{bmatrix}$$

provided $|\mathbf{M}| \neq 0$ and $|\mathbf{P}-\mathbf{O}\mathbf{M}^{-1}\mathbf{N}| \neq 0$, where $\mathbf{M}$ is an $n\times n$ diagonal matrix and $\mathbf{N}$, $\mathbf{O}$, and $\mathbf{P}$ are matrices of dimensions $n\times 3$, $3\times n$, and 3×3, respectively. Whereas $\mathbf{A}^T\mathbf{A}$ is a symmetric matrix, $\mathbf{P}$ has to be symmetric and $\mathbf{O}$ has to be equal to $\mathbf{P}$. This significantly reduces the computational burden.

6. SOME EXPERIMENTAL RESULTS

In this section some results are presented to demonstrate the performance of the proposed method. Most of the tests have been carried out using synthetic data since the motion of the scanner can be known exactly. In particular, the results presented

in this section are obtained from the scenario shown in Figure 3a. Another kind of scenario has provided similar results, except in some degenerate cases like an infinite wall or a long corridor, where one of the motion components becomes undetermined.

In the simulated experiments, we construct the sequence by scanning at fixed translational and rotational intervals (Δx, Δy, and $\Delta \phi$, respectively). At each position, the translational and rotational components of the displacement are computed by the proposed algorithm and the corresponding error (real minus computed) is recorded. Some plots showing the percentage errors obtained when using different number of range points are shown in Figure 3b and different displacements between scans are displayed in Figure 4.As expected, the larger the number of scanned points and the smaller the displacement, the better the results, that is, the error in the motion estimate depends on how close the discrete formulation is to the continuous case. In particular, Figure 4b reveals the strong influence of rotation in the performance of the algorithm. This is because, at long distances, even a small rotation produces many points near the corners to violate the velocity constraint equation. This fact has been verified through other experiments in which smooth contours yielded much better results because of the absence of corners.

The proposed algorithm also has been tested using real data provided by a laser range-finder. The sensor has a range resolution of 5 cm, an accuracy of ± 20 cm, and provides up to 360 measures in a 180° field of view. The experiment consists of taking 10 stationary scans at known equally separated positions with no rotation. Figure 5a shows the scans taken at the first and last position from the sequence. Figure 5b plots the errors for the nine displacements. In this case, the error plotted is not percentage, but real displacement minus computed displacement. As expected, the results become worse because the noise and truncation errors significantly affect the estimated derivatives. We do believe that these results can be significantly improved by integrating different scans as well as by discarding those range points where the spatial and temporal derivatives present discontinuities.

7. CONCLUSIONS AND FUTURE WORK

In this article, we have presented a new approach to recover the instantaneous motion of a radial laser range-finder along with the motion field of the range points in the scans. Experimental results showing that good results are achieved with both real and synthetic data have been presented. Although we have concentrated on estimating the motion parameters of the mobile robot, we think that the motion field can be very useful for a number of applications, including range image segmentation and object motion detection and tracking.

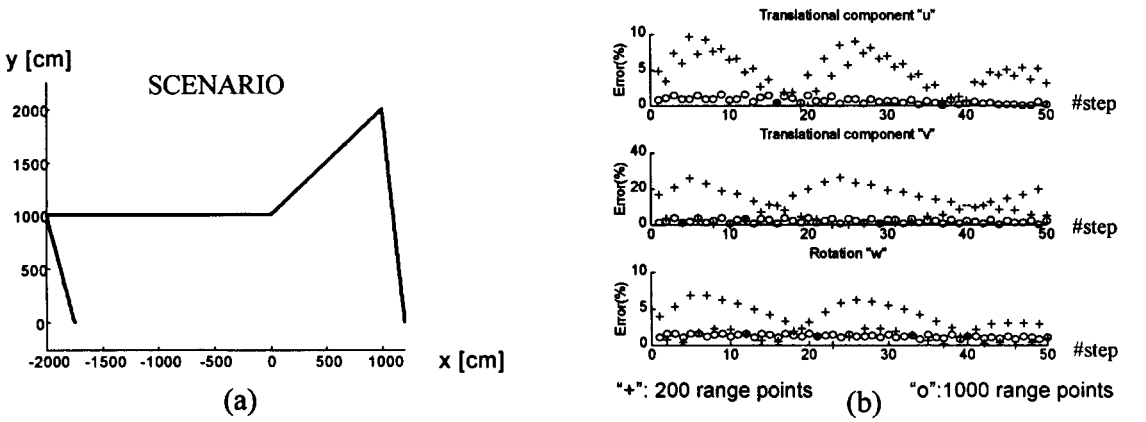

Figure 3. (a) Synthetic scenario used for the simulated tests. (b) Motion errors for two different numbers of range points. The real displacement was $\Delta x = 5$ cm, $\Delta y = 2$ cm, and $\Delta \phi = 0.01$ rad.

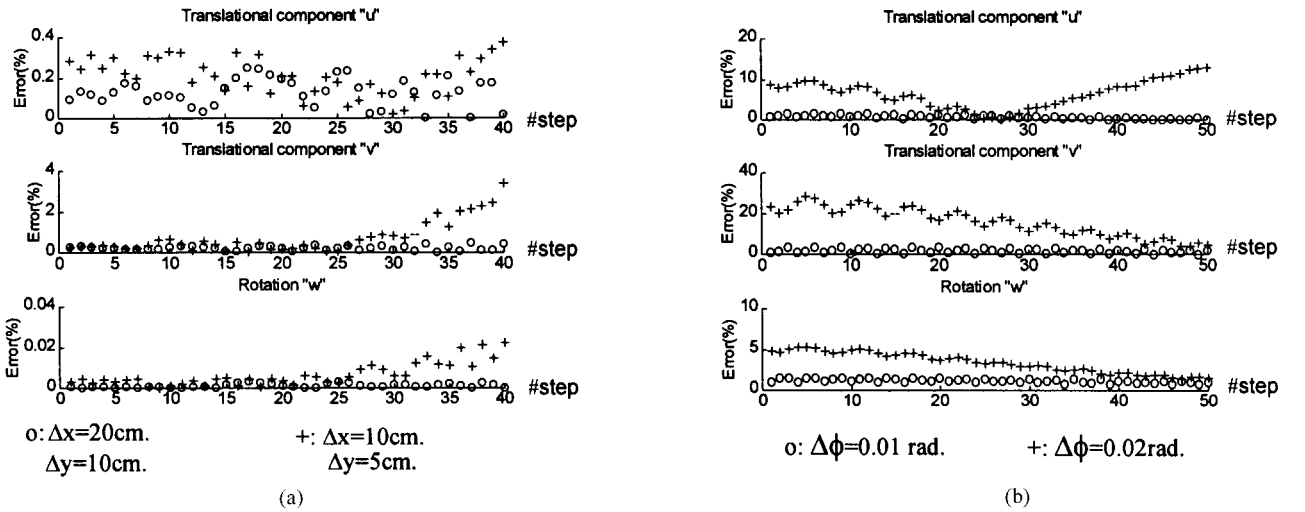

Figure 4. Errors in the displacement for a pure translation with two different translational parameters (a) and for two different rotational parameters and a translation of $\Delta x = 5$ cm, $\Delta y = 2$ cm (b). In both experiments the number of range points is 1000.

Currently, we are trying to improve the performance of the proposed algorithm by overcoming some limitations that have emerged from this preliminary work. The improvements include robustness to range data noise, integration of different scans by using, for example, a Kalman Filter, and automatically detecting and discarding those range points that violate the velocity constraint equation. We also plan to extend this formulation to 3D laser scanners.

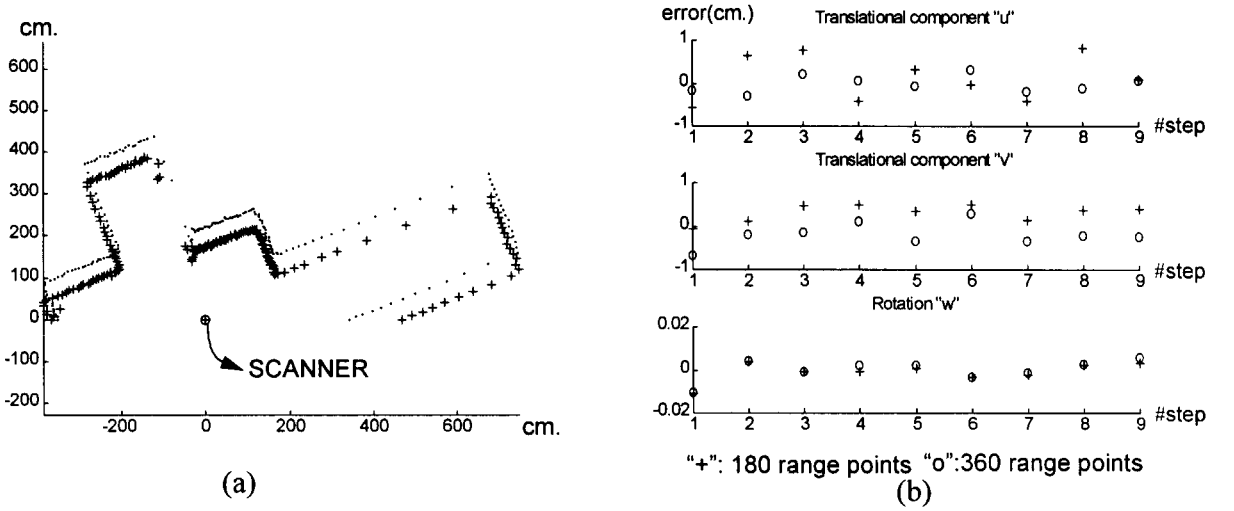

Figure 5. (a) Scans taken at the first and last position in a sequence. (b) Errors obtained for the nine displacements ($\Delta x = 5$ cm, $\Delta y = 2$ cm, $\Delta \phi = 0°$).

This work was supported by the Spanish Government under project CICYT-TAP96-0763.

REFERENCES

1. G. Shaffer, Two-dimensional mapping of expansive unkown areas, PhD dissertation, Carnegie Mellon University, Pittsburgh, 1995.
2. J. Gonzalez, A. Ollero, and A. Reina, Map building for a mobile robot equipped with a laser range scanner, IEEE International Conference on Robotics and Automation, San Diego, May 1994.
3. I.C. Cox, Blanche—An experiment in guidance and navigation of an autonomous robot vehicle, IEEE Trans Robotics Automat 7(2) (1991), 193–204.
4. J. Gonzalez, A. Stentz, and A. Ollero, A mobile robot iconic position estimator using a radial laser scanner, J Intell Robotic Systems 13 (1995), 161–179.
5. F. Lu, Shape registration using optimization for mobile robot navigation, PhD Dissertation, Univ. of Toronto, 1995.
6. B.K.P. Horn and B.G. Schunck, Determining optical flow, Artificial Intelligence 17 (1981), 185–203.
7. B.K.P. Horn and S. Negahdaripour, Direct passive navigation: Analytical solution for planes, IEEE Trans Pattern Anal Machine Intell 9(1) (1987), 168–176.
8. J.H. Mathew, Numerical methods for mathematics, science and engineering, 2nd ed., Prentice-Hall, Englewood Cliffs, NJ, 1992.
9. K. Ogata, Modern control engineering, 2nd ed., Prentice-Hall, Englewood Cliffs, NJ, 1990.